Korean J. Chem. Eng., **16**(5), 549-555 (1999)

Separation of CO_2 by 2-Amino-2-Methyl-1-Propanol Aqueous Solution in Microporous Hydrophobic Hollow Fiber Contained Liquid Membrane

Sang-Wook Park†, In-Joe Sohn, Dong-Soo Suh and Hidehiro Kumazawa*

Department of Chemical Engineering, College of Engineering, Pusan National University, Pusan 609-735, Korea
*Department of Chemical and Biochemical Engineering, Toyama University, Toyama 930-8555, Japan
(*Received 26 February 1999 • accepted 30 July 1999*)

Abstract–The absorption of CO_2 from a mixture of CO_2/N_2 gas was carried out using a flat-stirred vessel and the polytetrafluoroethylene hollow fiber contained aqueous 2-amino-2-methyl-1-propanol (AMP) solution. The reaction of CO_2 with AMP was confirmed to be a second order reversible reaction with fast-reaction region. The mass transfer resistance in the membrane side obtained from the comparison of the measured absorption rates of CO_2 in a hollow fiber contained liquid membrane with a flat-stirred vessel corresponded to about 90% of overall-mass-transfer resistance. The mass transfer coefficient of hollow fiber phase could be evaluated, which was independent of CO_2 loading.

Key words : Hollow Fiber Contained Liquid Membrane, Absorption, CO_2, 2-amino-2-methyl-1-propanol

INTRODUCTION

Nowadays the global warming issue caused by greenhouse gases has become a matter of great concern, and carbon dioxide, which is produced in enormous amounts, has been widely recognized as one of the greenhouse gases with the most influence. Many plants such as fossil-fuel-fired power plants, iron and steel works, and cement works discharge a huge amount of CO_2 day after day. The fixation and removal of CO_2 from fossil-fuel combustion facilities has been considered as a way to prevent CO_2 buildup. Chemical absorption and membrane based on separation are among the possible processes by which CO_2 can be successfully reduced from industrial waste gases and other gas mixtures.

Recently, a better and more attractive process was developed for CO_2 separation. It consists of module-like porous hollow fiber based contactors. Until a few years ago, these kinds of modules were only used for filtration purposes. However, recent work [Qi and Cussler, 1985; Karror and Sirkar, 1993] has confirmed that their use as gas-liquid contactors was also feasible. In these kinds of contacting devices several advantages can be encountered [Qi and Cussler, 1985; Yang and Cussler, 1986]; such as a larger interfacial area between gas and liquid flow, independent control of gas and liquid flow rates without flooding, loading or weeping problems, down sizing and the possibility of combining absorption and desorption in one single compact module and so on. The design of these kinds of contactors, however, remains limited by the resistance for mass transfer in the gas phase, liquid phase and the additional membrane phase.

Following the idea of using an immobilized liquid in the pores of a polymeric medium, a new type of membrane absorber such as hollow fiber contained liquid membrane (HFCLM) was developed in order to carry out simultaneously two processes of absorption and desorption. These contactors, which were first introduced by Majumdar et al. [1988], consisted of using the absorbent liquid in the shell side between feed-gas-carrying and sweep-gas-carrying fibers. The feasibility of gas purification in the HFCLM contactor was later investigated by Guha et al. [1992]. They focused mainly on the study of gas purification under several operational modes in order to find the optimum of the recovery of CO_2 in the CO_2/N_2 gas mixture, with either reactive or nonreactive liquid membranes. Their results confirmed the success and the flexibility of possible use of these systems in all modes without humidification of gas streams, confirming its use as a successful alternative to conventional methods for gas separation.

It is necessary to observe the resistance behavior in the hollow fiber phase in order to explain the mechanism of the mass transfer of CO_2 in a hollow fiber module.

In this study as a series of the first part of CO_2 separation in HFCLM [Park et al., 1997], the mechanism of absorption of CO_2 by aqueous solution of AMP in HFCLM was proposed, and the membrane-side-mass transfer resistance, which was obtained from a comparison of the measured absorption rates of CO_2 in HFCLM and those in a flat-agitated absorber, was investigated by the change of the experimental parameters such as the flow rate of gas mixture, the partial pressure of CO_2 in the feed gas mixture, the concentration of AMP and the loading of CO_2 in AMP.

THEORY

A theoretical model is developed here to describe the absorption of CO_2 from CO_2/N_2 mixture flowing in the tube into liquid through the pore of the porous hollow fiber, where bundles of the hollow fibers are soaked.

The following assumptions are utilized to set up the governing mass transfer differential equation: (1) the absorbent liquid

†To whom correspondence should be addressed.
E-mail : swparkϕ@hyowon.pusan.ac.kr

exists outside the tube and is mixed perfectly, (2) the mixture gases flow inside the tube with a plug flow and are ideal gas, (3) the pores of tube are filled with gas mixture, (4) the reaction of CO_2 with AMP in the absorbent liquid occurs outside the tubes and is a fast pseudo-first-order reaction, (5) steady-state and isothermal condition, (6) application of Henry's law, (7) no absorption of inert gas. Using these assumptions, the conservation equation for CO_2 flowing inside the tube is given by

$$\bar{v}\frac{dC_A}{dz}+\frac{A_{ti}}{V}\varepsilon N_i K_{AF}(P_A-P_A^*)=0 \tag{1}$$

Integrating Eq. (1) after converting the concentration of CO_2 in the tube, C_A to the partial pressure of CO_2, Eq. (1) using the assumption (1) is expressed as follows:

$$\ln\frac{(P_{A2}-P_A^*)}{(P_{A1}-P_A^*)}=\frac{-2RT\varepsilon N_i K_{AF}L}{r_i\bar{v}} \tag{2}$$

The overall mass transfer coefficient for absorption is defined like this,

$$N_{AF}=K_{AF}P_{ALM} \tag{3}$$

where

$$P_{ALM}=\frac{P_{A1}-P_{A2}}{\ln\left(\frac{P_{A1}-P_A^*}{P_{A2}-P_A^*}\right)}$$

It is necessary to get the physicochemical properties such as the diffusivity and solubility of CO_2 in AMP aqueous solution and the reaction rate constant of CO_2 with AMP for the theoretical value of the CO_2 flux in a flat-stirred vessel. Because the diffusivity and solubility of an acid gas in an aqueous phase were dependent on the ionic strength of electrolyte aqueous solutions [Danckwerts, 1970], these values were obtained from the empirical equation in the previous study [Park et al., 1997].

In the aqueous solution, CO_2 and AMP react according to the following overall reaction [Messaoudi and Sada, 1996];

$$CO_2(A)+RNH_2(B)+H_2O \underset{k_2'}{\overset{k_2}{\rightleftarrows}} HCO_3^-(E)+RNH_3^+(F) \tag{4}$$

The reaction of CO_2 with AMP was classified in the range of a fast reaction region and can be expressed like this [Doraiswamy and Sharma, 1984],

$$N_A=C_A^*\sqrt{k_2 D_A C_{Bo}} \tag{5}$$

The reaction rate constant (k_2) was used as 231 m^3/kmol·s [Park et al., 1997].

Since a chemical equilibrium exists in the reaction of CO_2 with AMP [Bosch et al., 1990], it is necessary to know the equilibrium concentration of CO_2 and various species in AMP aqueous solution at a fixed loading of CO_2 in order to get the theoretical value of CO_2 flux in a flat-stirred vessel, which will be discussed in the following section, and to analyze the performance of HFCLM.

The chemical equilibrium in systems comprised of CO_2, primary amines and water is governed by the following equations [Yih and Sen, 1988],

$$RNH_3^+ \rightleftarrows H^+ + RNH_2 \tag{6}$$

$$RNHCOO^- + H_2O \rightleftarrows RNH_2 + HCO_3^- \tag{7}$$

$$H_2O + CO_2 \rightleftarrows H^+ + HCO_3^- \tag{8}$$

$$H_2O \rightleftarrows H^+ + OH^- \tag{9}$$

$$HCO_3^- \rightleftarrows H^+ + CO_3^{2-} \tag{10}$$

Eqs. (6) and (7) represent the amine protonation and the amine carbamate hydrolysis, respectively. Eqs. (8)-(10) are the typical ionization reactions for aqueous systems containing CO_2. Since AMP has a tertiary carbon atom attached to the amino group, its carbamate is highly unstable and easily reverts to amine and bicarbonate. Toniwatchwuthikul et al. [1991] reported that carbamate ions could not be detected in CO_2 bearing AMP solutions, and they concluded that the bicarbonate and carbonate ions are the only major chemical sinks for CO_2.

The equilibrium constants representing the important reactions in the CO_2-AMP-H_2O system, in which water is present in excess, are given by

$$K_1=\frac{[H^+][RNH_2]}{[RNH_3^+]} \tag{11}$$

$$K_3=\frac{[H^+][HCO_3^-]}{[CO_2]} \tag{12}$$

$$K_4=[H^+][OH^-] \tag{13}$$

$$K_5=\frac{[H^+][CO_3^{2-}]}{[HCO_3^-]} \tag{14}$$

In addition to the above equilibrium equations, the overall material and charge balances must also be satisfied:

$$[AMP]=[RNH_2]+[RNH_3^+] \tag{15}$$

$$\alpha[AMP]=[CO_2]+[HCO_3^-]+[CO_3^{2-}] \tag{16}$$

$$[RNH_3^+]+[H^+]=[OH^-]+[HCO_3^-]+[CO_3^{2-}] \tag{17}$$

where [AMP] and α denote the total AMP concentrations and the CO_2 loading of the AMP solution, respectively.

The solubility of CO_2 in the liquid phase is governed by Henry's law:

$$P_A=H_A C_A \tag{18}$$

The equilibrium constants in Eqs. (11)-(14) and Henry's law constant were obtained from the reference [Toniwatchwuthikul et al., 1991];

$$K_3=\exp(-241.818+298.253\times10^3T^{-1}-148.528\times10^6T^{-2}+332.648\times10^8T^{-3}-282.394\times10^{10}T^{-4}) \tag{19}$$

$$K_4=\exp(39.5554-987.9\times10^2T^{-1}+568.828\times10^5T^{-2}-146.451\times10^8T^{-3}+136.146\times10^{10}T^{-4}) \tag{20}$$

$$K_5=\exp(-294.74+364.385\times10^3T^{-1}-184.158\times10^6T^{-2}+415.793\times10^8T^{-3}-354.291\times10^{10}T^{-4}) \tag{21}$$

$$H_A=\exp(22.2819-138.306\times10^2T^{-1}+691.346\times10^4T^{-2}-155.895\times10^7T^{-3}+120.037\times10^9T^{-4})/7.0061 \tag{22}$$

$$pK_1=2309.1+0.49828T-70850/T-388.03\ln T-6.3899C_A-0.095221\ln C_A+0.038508C_{Bo} \tag{23}$$

Eqs. (11)-(18) may be used to find the concentrations of

species in the AMP solution and the equilibrium partial pressure of CO_2 provided C_{Bo}, α, equilibrium constants and Henry's law constant.

EXPERIMENTAL

All chemicals in this study were reagent grade and were used without further purification. The hollow fibers used in this study were a microporous hydrophobic polytetrafluoroethylene (PTFE-21, Mitsubishi Co., outside diameter; 2 mm, inside diameter; 1 mm, porosity; 50%, mean pore size; 0.20 μm).

The rates of absorption into AMP aqueous solution were measured by using a flat-stirred vessel and an HFCLM as reported before [Park et al., 1997].

A bundle of 7 fibers with 0.6 m length of each fiber was used for absorption in HFCLM. The volume of absorbent liquid in the vessel was 7×10^{-4} m^3. CO_2 diluted with N_2 was fed to the lumen side of the hollow fibers for absorption, and the gas composition was adjusted by using the mass flow controller. The gas mixture was saturated with water. The absorption temperature was controlled by an air-bath. The compositions of CO_2 at inlet and outlet of the bundle were analyzed by a gas chromatograph (Shimadzu GC-8A, TCD, packing material; Porapak Q, detector temperature; 130 °C, the flow rate of carrier gas, He; 3.3×10^{-7} m^3/s), and flow rates of outlet were measured by a soap-bubbler. The absorbent liquid was stirred with an agitator, and the concentration of AMP was measured by HCl titration.

The range of flow rate of gas mixture ws 3.3×10^{-7}-1.67×10^{-6} m^3/s, those of composition of CO_2 in feed gases of CO_2-N_2 mixture, 1-13 mole%, those of concentration of AMP as absorbent agent, 0.5-2 $kmol/m^3$, those of agitation speed, 150-500 rev/min and loading of CO_2 in AMP aqueous solution, 0-0.75, and absorption experiments were carried out at 25 °C and atmospheric pressure.

The mass transfer rates of CO_2 transferred from tube side into the absorbent liquid were obtained from the differences of composition of CO_2 and flow rates between inlet and outlet of tubes at steady-state condition.

RESULTS AND DISCUSSION

1. Absorption of CO_2 in a Flat-stirred Vessel

The theoretical value of N_{AS} is required to classify the overall reaction between CO_2 and AMP as shown in Eq. (4) in the AMP aqueous solution loaded with CO_2.

The film model accompanied with a chemical reaction can be written as follows:

$$D_j\frac{d^2C_j}{dx^2}=-R_j \tag{24}$$

where,

$$R_j=k_2C_AC_B-\frac{k_2}{K}C_EC_F \tag{25}$$

with the following boundary conditions:

$$x=0;\ P_A=H_AC_A,\ \frac{dC_j}{dx}=0 (j=B,\ E\ or\ F)$$

$$x=\delta;\ C_j=C_{j.eq} (j=A,\ B,\ E\ or\ F)$$

The overall equilibrium constant, K is defined as follows,

$$K=\frac{K_3}{K_1} \tag{26}$$

The equilibrium concentration of j species was calculated from the Eqs. (11)-(18) at the given values of C_{Bo}, P_A and α.

The absorption rate of CO_2 into the AMP aqueous solution in a flat-stirred vessel is expressed as follows:

$$N_{AS}=-D_A\frac{dC_A}{dx}\bigg|_{x=0} \tag{27}$$

The absorption rates of CO_2 into AMP solution in a flat-stirred vessel were measured according to the change of partial pressure of CO_2 and the concentration of AMP at various CO_2 loading. Fig. 1 shows the relationship between the absorption rate of CO_2 and the partial pressure of CO_2, where the initial concentration of AMP is 1 $kmol/m^3$, the partial pressure of CO_2 is varied from 0.015 to 0.12 atm at various CO_2 loading between 0.2 to 0.75 and gas flow rate of 1×10^{-6} m^3/s. The relationship between these two factors on a logarithmic scale can be described by straight lines with a slope of unity at loadings below 0.4. At the loading of 0.75, the absorption rate is abruptly decreased as the partial pressure decreases below about 0.07 atm.

As shown in Fig. 1, the absorption rate decreases with increasing CO_2 loading. Below 0.75 of the loading, the absorption rate is proportional to the partial pressure of CO_2. This behavior arises from the fact that the partial pressure is much higher than the equilibrium pressure of CO_2 for the loaded AMP solution. At CO_2 loading of 0.75, the equilibrium pressure is evaluated to be 0.051 atm from Eqs. (11)-(18). Accordingly, the absorption rate decreases at CO_2 partial pressure below 0.07 atm as depicted in Fig. 1.

In Fig. 1, both observed and predicted value of absorption rate are plotted together for the purpose of comparison. It is

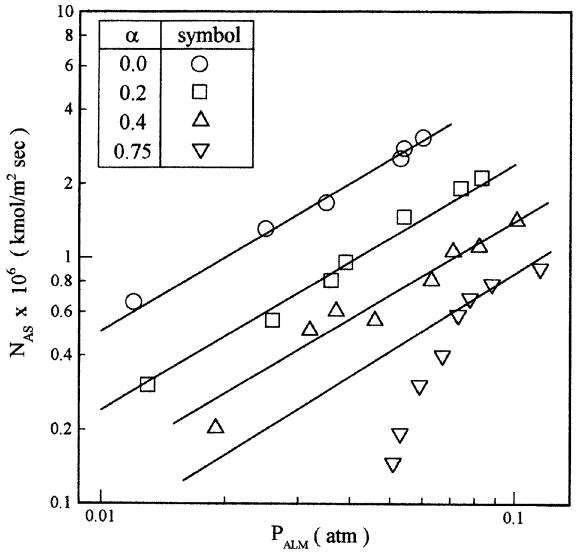

Fig. 1. Effect of partial pressure of CO_2 on absorption rate of CO_2 with flat-stirred vessel.
(C_{Bo}=1 $kmol/m^3$, Q_{in}=1×10^{-6} m^3/s)

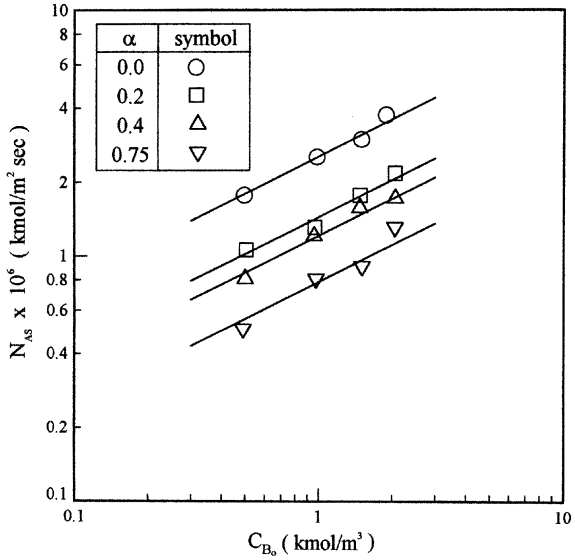

Fig. 2. Effect of concentration of AMP on absorption rate of CO_2 with flat-stirred vessel.
(Q_{in}=1×10^{-6} m^3/s, P_{A1}=0.1 atm)

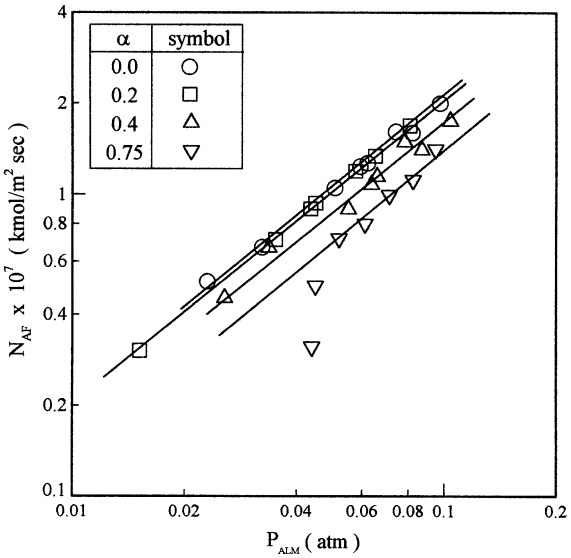

Fig. 3. Absorption rate of CO_2 in HFCLM.
(C_{Bo}=1 kmol/m^3, Q_{in}=1×10^{-6} m^3/s)

seen that a relatively good agreement is found between measured and calculated value of absorption rate of CO_2 for loading up to 0.4. This confirms that the reversibility of reaction (4) is no influence on the reaction rate constants determined under the assumption of a fast reaction region within the range of the experimental condition investigated.

Fig. 2 shows a plot of the measured and calculated value of absorption rate of CO_2 against the AMP concentration at the various CO_2 loading at a gas flow rate of 1×10^{-6} m^3/s and partial pressure of CO_2 at the inlet of 0.1 atm. It is seen that the calculated absorption rate of CO_2 approaches reasonably to the measured one, and the relationship between the absorption rate and AMP concentration can be expressed by straight lines with a slope of 0.5.

It is concluded that the reaction of CO_2 with AMP belongs to the fast reaction region from a comparison of Eq. (5) with the slopes of the straight line in Figs. 1 and 2.

2. Absorption of CO_2 in HFCLM

The rates of absorption of CO_2 were measured by the change of the partial pressure of CO_2, gas flow rate and the concentration of AMP at various loadings of CO_2. The rate of absorption of CO_2 was plotted against the logarithmic mean of the partial pressure of CO_2 in Fig. 3 in the range of the partial pressure of CO_2 at the inlet from 0.03 to 0.13 atm and the CO_2 loading from 0.2 to 0.75 at the flow rate of gas mixture of 1×10^{-6} m^3/s and AMP concentration of 1 kmol/m^3. The logarithmic mean partial pressure of CO_2 was calculated using the measured partial pressure of CO_2 at the inlet and the outlet, and the equilibrium partial pressure of CO_2 obtained from Eqs. (11)-(18). As shown in Fig. 3, the rate of CO_2 absorption tends to decrease with increasing CO_2 loading, and to increase with increasing of the logarithmic mean of partial pressure of CO_2. The plots between N_{AF} and P_{ALM} were linear and their slope was unity except CO_2 loading of 0.75. The behavior of the nonlinearity between the absorption rate and the partial pressure of CO_2 might be explained with the similar result of the flat-stirred vessel as shown in Fig. 1.

Fig. 4 shows a plot of the rate of absorption of CO_2 against the logarithmic mean of the partial pressure of CO_2 in the range of AMP concentration from 0.5 to 2.0 kmol/m^3 at CO_2 loading of 0.2. As shown in Fig. 4, the rate of absorption of CO_2 was increased with increasing AMP concentration and the logarithmic mean of the partial pressure of CO_2. In order to get the relationship between the absorption rate of CO_2 and the AMP concentration, the absorption rates of CO_2 were plotted against the AMP concentration at CO_2 loading of 0.2 and the partial pressure of CO_2 at the inlet of 0.1 atm in Fig. 5, where the relationship between these two variables can be treated by a straight line with the slope of 0.5.

In order to get the effect of gas flow rate on the absorption rate of CO_2, Fig. 6 shows a plot of the rate of CO_2 absorption

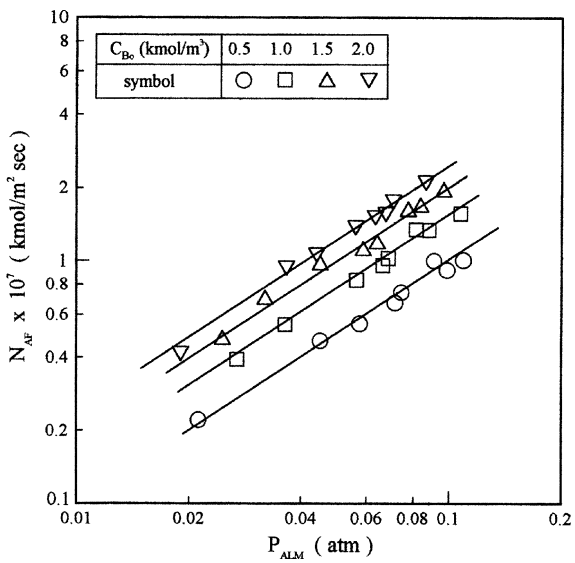

Fig. 4. Absorption rate of CO_2 in HFCLM.
(Q_{in}=1×10^{-6} m^3/s, α=0.2)

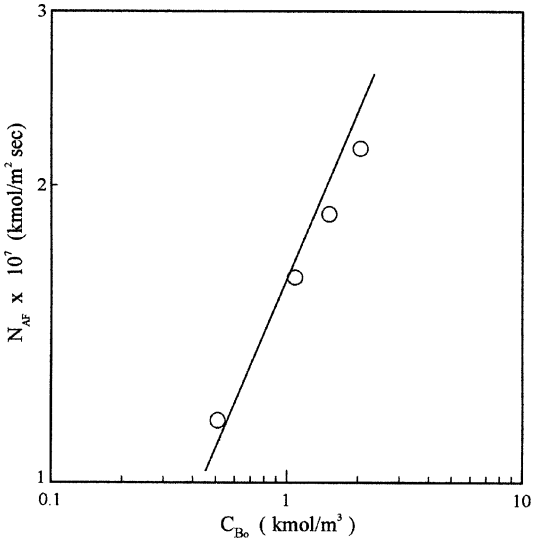

Fig. 5. Effect of concentration of AMP on mass transfer rate of absorption.
(Q_{in}=1×10^{-6} m^3/s, P_{A1}=0.1 atm, α=0.2)

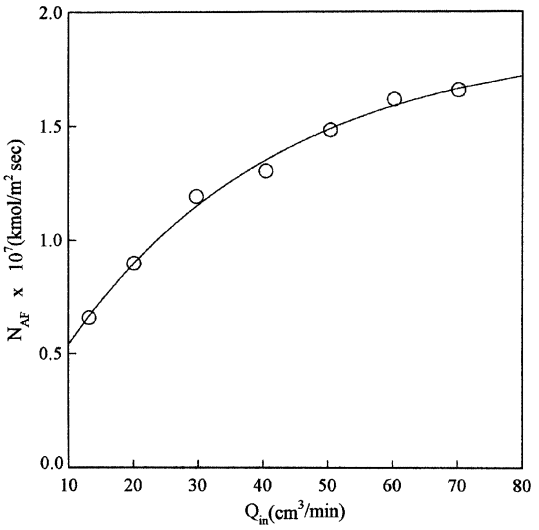

Fig. 6. Effect of gas flow rate on absorption rate of CO_2.
(α=0.4 C_{Bo}=1 kmol/m^3, P_{A1}=0.1 atm)

against the flow rate of the gas mixture in the range of gas flow rate from 15 to 65 cm^3/min. As shown in Fig. 6, the rate of CO_2 absorption was increased with increasing of the flow rate of gas mixture. As shown in Eq. (2), the partial pressure of CO_2 at the outlet was increased with increasing of the flow rate. Therefore, the rate of absorption of CO_2 should be decreased, but the experimental results were contrary as shown in Fig. 6. This might be explained as that the mass transfer resistance has more influence on the flux than the resistance time of gas in the tube as the gas flow rate increases.

3. The Mass Transfer Resistance of the Hollow Fiber Phase

In order to observe the characteristics of the HFCLM, we plotted the measured absorption rates of CO_2 in the flat-stirred vessel and HFCLM against the logarithmic mean of partial pressure of CO_2 at CO_2 loading of 0.4 in Fig. 7, respectively. A tendency of increasing of N_{AF} with increasing of P_{ALM} represents a similar behavior in the flat-stirred vessel, and the absorption rate in HFCLM is found to be lower by about an order of magnitude than that in the flat-stirred vessel. It has been confirmed that the absorption process in the flat-stirred vessel with a plane gas-liquid interface is controlled by diffusion accompanied by chemical reaction in the liquid phase; on the other hand, the absorption of CO_2 in HFCLM might be governed by the resistance in the liquid and hollow fiber phases.

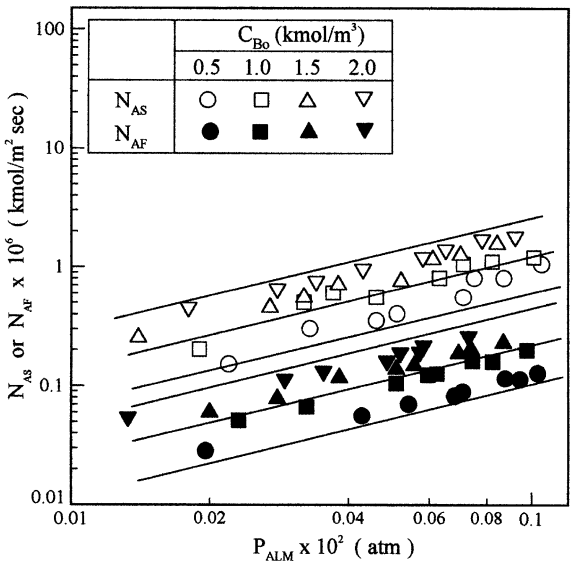

Fig. 7. Absorption rates of CO_2 in a flat-stirred vessel and HFCLM at α=0.4.

The overall mass transfer coefficient is defined as follows:

$$N_{AS}=K_{AS}P_{ALM} \tag{28}$$

The mass transfer in the flat-stirred vessel and the hollow fiber mode described in terms of a resistance-in-series model can be written as follows, respectively:

$$\frac{1}{K_{AS}}=\frac{1}{k_G}+\frac{H_A}{k_L} \tag{29}$$

$$\frac{1}{D_e K_{AF}}=\frac{1}{D_i k_G}+\frac{1}{D_i k_m}+\frac{H_A}{D_o k_L} \tag{30}$$

If it is assumed that the liquid-phase resistance is equal to the total resistance in the flat-stirred vessel, the resistance of hollow fiber phase can be evaluated as follows:

$$R_M=R_F-R_S \tag{31}$$

where, R_F and R_S are the reciprocal number of the overall mass transfer coefficient obtained from Eqs. (3) and (28), respectively.

Fig. 8 shows the resistances of the flat-stirred vessel, HFCLM, and hollow fiber phase against the AMP concentration at CO_2 loading of 0.2. As shown in Fig. 8, these three kinds of mass transfer resistance were slightly decreased with increasing of AMP concentration, and the amount of the resistance of hollow fiber phase is as large as about 90% of the total resistance of HFCLM. If non-wetted pore prevails in the hollow fiber phase, the physical diffusion of the gas phase in the pore should be taken place. Accordingly, the hollow fiber phase resistance must be independent of AMP concentration. But, as shown in

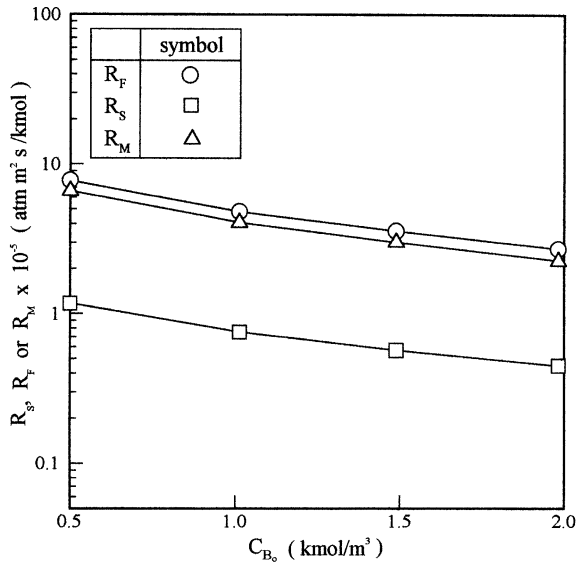

Fig. 8. Effect of AMP concentration on the mass transfer resistances of a flat-stirred vessel, HFCLM and hollow-fiber phase at α=0.4.

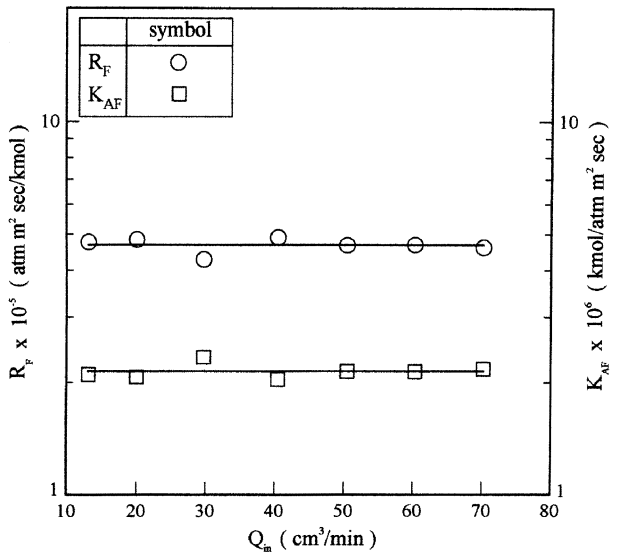

Fig. 9. Effect of gas flow rate on R_F and K_{AF}. (α=0.4, C_{Bo}=1 kmol/m^3, P_{A1}=0.1 atm)

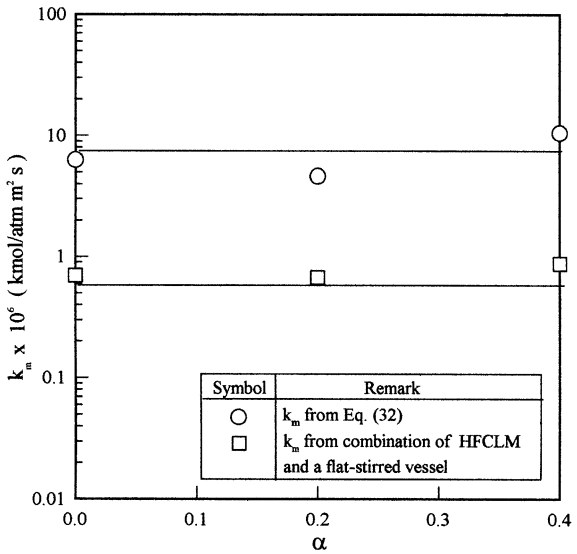

Fig. 10. Comparison of k_m of Eq. (32) with k_m from combination of HFCLM and a flat-stirred vessel.

Fig. 8, the hollow fiber resistance tended to decrease with increasing AMP concentration because conceivably the aqueous AMP solution partially leaks into pores of the hollow fiber phase, and the hollow fiber phase here is governed by liquid-phase diffusion with reaction.

In order to observe the resistance in gas phase, the overall mass transfer coefficient and resistance were plotted against the gas flow rate in Fig. 9 by using Eq. (3) at α, 0.4, C_{Bo}, 1 kmol/m^3, and P_{A1}, 0.1 atm. As shown in Fig. 9 the overall mass transfer resistance is independent of the gas flow rate; therefore, Eq. (30) can be rearranged,

$$\frac{1}{D_e K_{AF}} = \frac{1}{D_i k_m} + \frac{H_A}{D_o k_L} \tag{32}$$

On the other hand, from a comparison of the mass transfer rate such as Eq. (5) with the rate of physical mass transfer, the liquid side mass transfer coefficient, k_L can be given as follows:

$$k_L = \sqrt{k_2 D_A C_{Bo}} \tag{33}$$

The mass transfer coefficient of the hollow fiber phases, k_m, can be obtained as a reciprocal number of R_M at C_{Bo}=0 in Fig. 8, or from Eq. (32) with Eq. (33). The values of k_m obtained by these two methods were plotted against the CO_2 loading in Fig. 10. The straight lines in this figure represent the average value of k_m. As shown in Fig. 10, k_m is independent of the CO_2 loading. This is explained by the fact that the hollow fiber resistance to diffusion in non-wetted pore is governed by physical diffusion. The difference of the values of k_m obtained by these two methods may be caused by the characteristics of the hydrodynamic behavior in the gas-liquid contactor such as the flat-stirred vessel and the hollow fiber mode.

CONCLUSION

The absorption of CO_2 from a mixture of CO_2/N_2 gas was carried out using the flat-stirred vessel and the polytetrafluoroethylene porous hollow fiber contained AMP aqueous solution. The overall reaction between CO_2 and AMP loaded with CO_2 was classified as a fast reaction region from a comparison of the measured and calculated absorption rate of CO_2 in a flat-stirred vessel. The measured absorption rate of CO_2 in HFCLM by varying the partial pressure of CO_2 from 0.03 to 0.12 atm, AMP concentration from 0.5 to 0.2 kmol/m^3, and CO_2 loading from 0.2 to 0.75 was found to be increased with increasing of the partial pressure of CO_2 and AMP concentration, and with decreasing of the CO_2 loading. The mass transfer resistance of the hollow fiber phase obtained from a comparison of the measured absorption rate of CO_2 in the flat-stirred vessel and HFCLM corresponded to about 90% of the overall mass transfer resistance. It was also observed that this value was not influenced by CO_2 loading, but slightly decreased with increasing of AMP

concentration within a limited range.

NOMENCLATURE

A : CO_2 species
A_{ti} : surface area of tube inside [m^2]
C_A : concentration of CO_2 in bulk body of liquid in a stirred vessel [kmol/m^3]
C_A^* : solubility of CO_2 in liquid [kmol/m^3]
C_B : concentration of AMP [kmol/m^3]
D_A : diffusivity of CO_2 in AMP aqueous solution [m^2/s]
D_i : inside diameter of tube [m]
D_o : outside diameter of tube [m]
D_e : equivalent diameter of tube as $\left(\frac{1}{1-\varepsilon}\right)^{1/2} D_o$ [m]
H_A : Henry constant of CO_2 in liquid [atm·m^3/kmol]
K : overall equilibrium constant defined in Eq. (26)
K_{AF} : overall mass transfer coefficient in HFCLM [kmol/m^2·s·atm]
K_{AS} : overall mass transfer coefficient in flat-stirred vessel [kmol/m^2·s·atm]
k_2 : forward reaction rate constant in Eq. (9) [m^3/kmol·s]
k_2' : backward reaction rate constant in Eq. (9) [s^{-1}]
k_G : gas-side mass transfer coefficient [kmol/m^2·s·atm]
k_m : membrane-side mass transfer coefficient [kmol/m^2·s·atm]
k_L : liquid-side mass transfer coefficient [m/s]
L : length of tube [m]
N_A : mass transfer rate of CO_2 [kmol/m^2·s]
N_{AS} : absorption rate of CO_2 in flat-stirred vessel [kmol/m^2·s]
N_f : number of tube [-]
P_A : partial pressure of CO_2 in tube inside [atm]
P_A^* : equilibrium partial pressure of CO_2 equivalent to C_A [atm]
P_{ALM} : logarithmic mean partial pressure of CO_2 [atm]
R : gas constant [atm·m^3/kmol·K]
R_j : reaction rate of j species defined in Eq. (25) [kmol/m^3·s]
R_F : overall mass transfer resistance in HFCLM [m^2·s·atm/kmol]
R_M : mass transfer resistance of hollow fiber phase [m^2·s·atm/kmol]
R_S : overall mass transfer resistance in flat-stirred vessel [m^2·s·atm/kmol]
r_i : radius of tube inside [m]
T : temperature [K]
V : volume of tube inside [m^3]
$\bar{v}$: mean velocity of gas in the tube [m/s]
x : radial distance in the tube [m]
z : position of tube [m]

Greek Letters

α : CO_2 loading defined as moles of CO_2 dissolved per mole of AMP in the aqueous solution [-]
δ : film thickness in liquid side for the film model [m]
ε : porosity of membrane

Subscripts

j : species
A : CO_2
B : RNH_2
E : HCO_3^-
eq : equilibrium condition
F : RNH_3^+ or HFCLM
o : initial value
S : flat-stirred vessel

REFERENCES

Bosch, H., Versteeg, G. F. and Vanswaaij, W. P. M., "Kinetics of the Reaction of CO_2 with the Sterically Hindered Amine 2-Amino-2-Methyl-1-Propanol at 298 K," *Chem. Eng. Sci.*, **45**, 1167 (1990).

Danckwerts, P. V., "Gas-Liquid Reactions," McGraw-Hill, New York (1970).

Doraiswany, L. K. and Sharma, M. M., "Heterogeneous Reaction: Analysis, Examples and Reactor Design," John Wiley & Sons, New York, **2**, 22 (1984).

Guha, A. K., Majumdar, S. and Sirkar, K. K., "Gas Separation Modes in a Hollow Fiber Contained Liquid Membrane Permeator," *Ind. Eng. Chem. Res*., **31**, 593 (1992).

Karoor, S. and Sirkar, K. K., "Gas Absorption Studies in Microporous Hollow Fiber Membrane Modules," *Ind. Eng. Chem. Res.*, **32**, 674 (1993).

Majumdar, S., Guha, A. K. and Sirkar, K. K., "A New Liquid Membrane Technique for Gas Separation," *AIChE J*., **34**, 1135 (1988).

Messaoudi, B. and Sada, E., "Kinetics of Absorption of Carbon Dioxide into Aqueous Solutions of Sterically Hindered 2-Amino-2-Methyl-1-Propanol," *J. Chem. Eng. Japan*, **29**, 193 (1996).

Park, S. W., Suh, D. S., Hwang, K. S. and Kumazawa, H., "Gas Absorption of Carbon Dioxide in a Hollow Fiber Contained Liquid Membrane Absorber," *Korean J. Chem. Eng*., **14**, 285 (1997).

Qi, Z. and Cussler, E. L., "Microporous Hollow Fiber for Gas Absorption, 1. Mass Transfer in the Liquid," *J. Membr. Sci*., **23**, 321 (1985).

Toniwatchwuthikul, P., Meisen, A. and Lim, C. J., "Solubility of CO_2 in a 2-Amino-2-Methyl-1-Propanol Solution," *J. Chem. Eng. Data*, **36**, 130 (1991).

Yang, M. C. and Cussler, E. L., "Designing Hollow Fiber Contactors," *AIChE J*., **32**, 1910 (1986).

Yih, S. and Sen, K., "Kinetics of Carbon Dioxide Reaction with Sterically Hindered 2-Amino-2-Methyl-1-Propanol Aqueous Solutions," *Ind. Eng. Chem. Res*., **27**, 2237 (1988).